

PAPER • OPEN ACCESS

Ultrathin transparent Copper(I) oxide films grown by plasma-enhanced atomic layer deposition for Back-end-of-line p-Type transistors

To cite this article: Hagyoul Bae *et al* 2021 *Nano Ex.* 2 020023

View the [article online](#) for updates and enhancements.

A promotional banner for the 240th ECS Meeting. The banner features a colorful striped border at the top. On the left, the ECS logo is displayed in a green circle. To its right, the text reads "240th ECS Meeting" in large blue font, followed by "Digital Meeting, Oct 10-14, 2021" in a smaller black font. Below this, it says "Register early and save up to 20% on registration costs" in bold black text, and "Early registration deadline Sep 13" in a smaller black font. At the bottom left, there is a red "REGISTER NOW" button. On the right side of the banner, there is a photograph of a diverse group of people in professional attire, smiling and interacting in a meeting setting.

ECS **240th ECS Meeting**
Digital Meeting, Oct 10-14, 2021
**Register early and save
up to 20% on registration costs**
Early registration deadline Sep 13
REGISTER NOW



PAPER

Ultrathin transparent Copper(I) oxide films grown by plasma-enhanced atomic layer deposition for Back-end-of-line p-Type transistors

OPEN ACCESS

RECEIVED
13 February 2021REVISED
10 May 2021ACCEPTED FOR PUBLICATION
13 May 2021PUBLISHED
10 June 2021

Original content from this work may be used under the terms of the [Creative Commons Attribution 4.0 licence](#).

Any further distribution of this work must maintain attribution to the author(s) and the title of the work, journal citation and DOI.

Hagyoul Bae^{1,2,*} , Adam Charnas^{1,2}, Wonil Chung^{1,2}, Mengwei Si^{1,2}, Xiao Lyu^{1,2}, Xing Sun³, Joon Park², Haiyan Wang³ , Dmitry Zemlyanov² and Peide D Ye^{1,2,*}¹ Electrical and Computer Engineering, Purdue University, West Lafayette, Indiana 47907, United States of America² Birk Nanotechnology Center, Purdue University, West Lafayette, Indiana 47907, United States of America³ Materials Engineering, Purdue University, West Lafayette, Indiana 47907, United States of America

* Authors to whom any correspondence should be addressed.

E-mail: hagyoulbae@gmail.com and yep@purdue.edu

Keywords: PEALD, Copper(I) oxide, thin-film transistors, density-of-states, p-Type oxide

Abstract

We demonstrate p-type thin-film transistors (TFTs) on copper(I) oxide (Cu₂O) grown by plasma-enhanced atomic layer deposition (PEALD) with bis(N,N'-di-sec-butylacetamido)dicopper(I) as the Cu precursor and oxygen (O₂) plasma as an oxidant. PEALD provides many of the advantages of other ALD processes, including uniformity and conformality, but with the additional ability to actively generate reactants and to add substantial energy from the plasma which may be important in defect control, low-temperature deposition. In this letter, Cu₂O films were grown on SiO₂/Si substrates under different substrate temperatures (160 ~ 240 °C) and post-deposition annealing was carried out under various temperatures (300 ~ 1100 °C) to improve the growth rate and crystallinity of the Cu₂O films. The fabricated p-channel bottom-gate Cu₂O transistors with a controlled thickness of 12 nm have high transparency over 90% and exhibit a subgap density of states ($g(E)$) of $7.2 \times 10^{18} \text{ eV}^{-1} \cdot \text{cm}^{-3}$ near the valence band (E_V), contact resistivity (R_C) of $14 \text{ k}\Omega \cdot \text{mm}$, I_{ON}/I_{OFF} ratio of 2×10^3 , and field-effect mobility of $0.1 \text{ cm}^2/\text{V}\cdot\text{s}$.

1. Introduction

Cu₂O is regarded as one of the most promising materials for achieving p-type transition metal oxide (TMO) thin-film transistors (TFTs) [1–4]. Furthermore, to enable monolithic three-dimensional (M3D) integration of high performance logic, high mobility n-type and p-type oxide semiconductor thin films that can be utilized for fabrication of back-end-of-line (BEOL) compatible complementary metal oxide semiconductor (CMOS) circuits are strongly demanded [5–8]. Cu₂O is natively p-type owing to the presence of Cu vacancies, which introduce an acceptor level near valence band edge E_V [9]. Cu₂O itself has a cubic structure with a direct bandgap of 2.1 ~ 2.5 eV [10]. Cu₂O films can be formed by a variety of methods such as sputtering [11–13], spray coating [14], solution process [15], pulsed laser deposition [16], chemical vapor deposition [17], and thermal oxidation [18]. Among these deposition techniques, atomic layer deposition (ALD) is particularly suitable for oxide thin-film growth due to its conformal step coverage and accurate thickness control [19]. Although ALD-based Cu₂O studies have been extensively reported [20–24], the fabrication and performance of PEALD-based Cu₂O TFTs has not been demonstrated to date.

Above all, an oxygen plasma or ozone process can play an important role in the improvement of chemical reactivity and film growth rate, which is the limitation for ALD of Cu₂O [25].

In this work, we present p-type TFTs fabricated on Cu₂O ultrathin films grown by PEALD process for the first time. We characterized device electrical performance including R_C , $g(E)$, and μ_{FE} as well as material properties such as phase composition, energy bandgap, and transmittance of the fabricated Cu₂O TFTs, although the quality of the materials and device fabrication process need to be further improved.

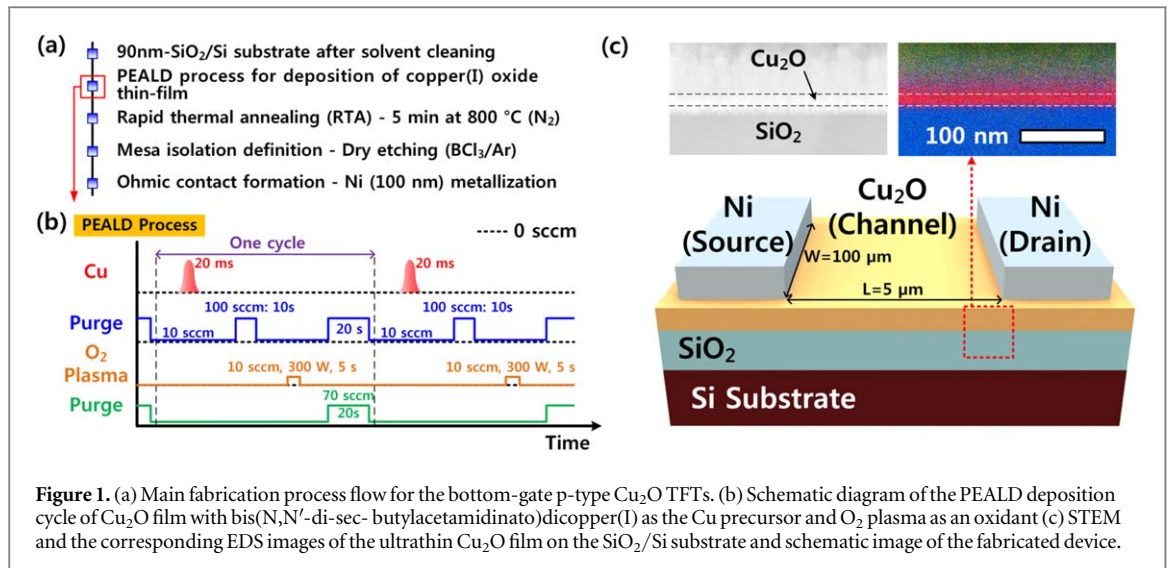


Figure 1. (a) Main fabrication process flow for the bottom-gate p-type Cu₂O TFTs. (b) Schematic diagram of the PEALD deposition cycle of Cu₂O film with bis(N,N'-di-sec-butylacetamido)dicopper(I) as the Cu precursor and O₂ plasma as an oxidant (c) STEM and the corresponding EDS images of the ultrathin Cu₂O film on the SiO₂/Si substrate and schematic image of the fabricated device.

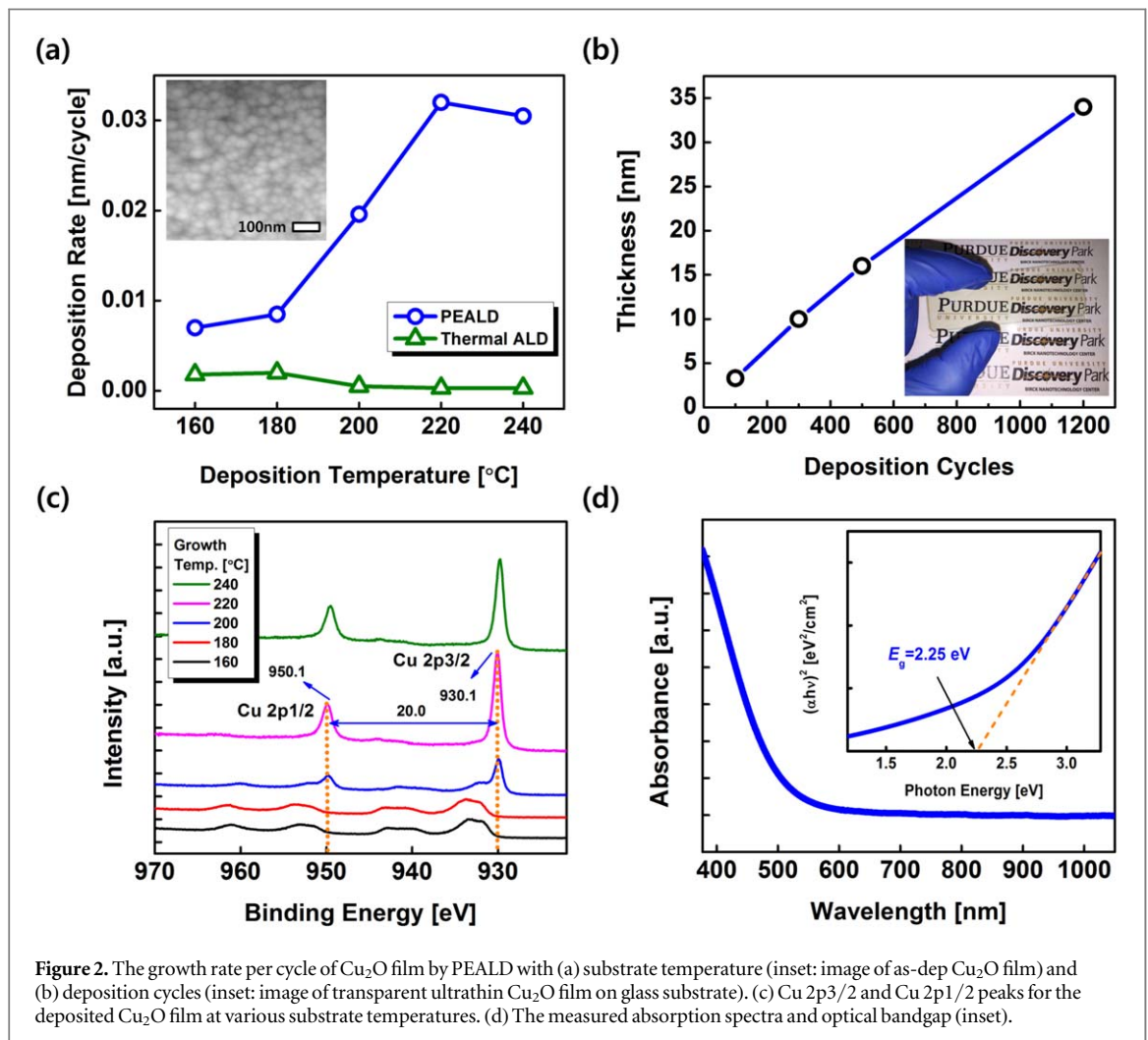
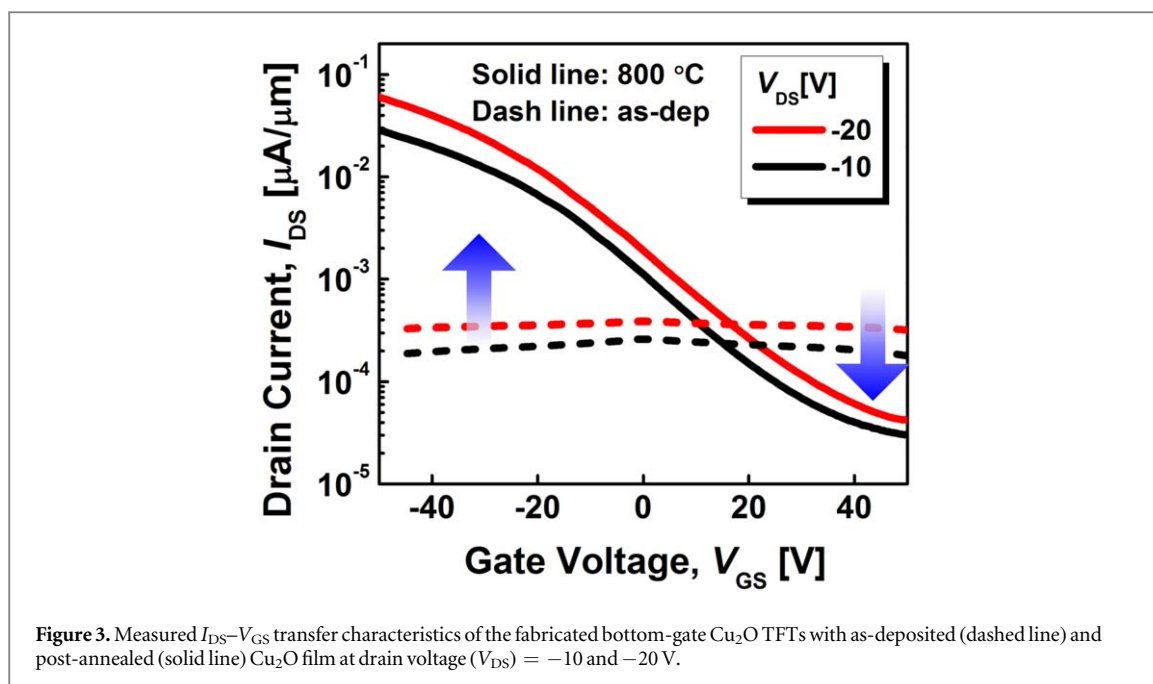


Figure 2. The growth rate per cycle of Cu₂O film by PEALD with (a) substrate temperature (inset: image of as-dep Cu₂O film) and (b) deposition cycles (inset: image of transparent ultrathin Cu₂O film on glass substrate). (c) Cu 2p_{3/2} and Cu 2p_{1/2} peaks for the deposited Cu₂O film at various substrate temperatures. (d) The measured absorption spectra and optical bandgap (inset).

2. Experiment

Figure 1(a) shows the key fabrication steps for the bottom-gate p-type Cu₂O TFTs on SiO₂/Si substrates using the newly developed PEALD process. The Cu₂O channel material was deposited by PEALD on SiO₂ (90 nm)/p + Si wafer, which was functioned as a bottom-gate. In this study, we used bis(N,N'-di-sec-butylacetamido)dicopper(I)[Cu(⁵Bu-Me-amd)]₂ as the Cu precursor [20]. The Cu precursor with the solid phase was



supplied by STREM, a company that produces a variety of high quality precursors for ALD process. As shown in figure 1(b), the optimized process consists of a Cu-precursor pulse for 20 ms with a 10 sccm N_2 flow, a purge pulse of 10 s with 100 sccm of N_2 flow, an O_2 plasma pulse for 5 s with 10 sccm under a plasma power of 300 W, and a purge pulse of 20 s with both 70 sccm of N_2 flow in main chamber and 100 sccm of N_2 flow in the plasma gas line. Next, rapid thermal annealing (RTA) at 800 °C was carried out under N_2 atmosphere for 5 min.

To define the Cu_2O channel region, we carried out mesa isolation using a BCl_3/Ar gas mixture in an inductively coupled plasma-reactive ion etching (ICP-RIE) system (Panasonic E620 Etcher) for 5 min. The etching rate of Cu_2O film is about 4 nm min^{-1} under the process conditions used: RF power of 100 W; BCl_3 flow of 15 sccm; Ar flow of 60 sccm; pressure of 0.6 Pa. Subsequently, Ni with a thickness of 100 nm was deposited for formation of source (S) and drain (D) contacts via an electron beam evaporator. A schematic view of the p-type Cu_2O TFTs with the bottom-gate structure is shown in figure 1(c). The fabricated device has the channel width (W) of 100 μm and length (L) of 5 μm .

3. Results and discussion

To increase the deposition rate and conductivity of the atomic layer deposited (ALD) Cu_2O film, we employed PEALD process under various conditions. Figure 2(a) shows the dependence of deposition rate on deposition temperature from 160 to 240 °C. The deposition rate rapidly increases with increasing deposition temperature until 220 °C. As shown in figure 2(b), a growth per cycle (GPC) of 0.33 Å was found for a substrate temperature of 220 °C. The inset of figure 2(b) shows a PEALD-grown transparent Cu_2O film with a thickness of 12 nm on a glass substrate. Figure 2(c) shows X-ray photoelectron spectroscopy (XPS) spectra of as-deposited Cu_2O films with various deposition temperatures between 160 to 240 °C. All the samples grown between 200 to 240 °C showed the characteristic Cu 2p_{3/2} and Cu 2p_{1/2} peaks at 950.1 and 930.1 eV, respectively. Figure 2(d) shows the high measured absorption spectra of the Cu_2O film, resulting in a high transparency of approximately 90%, corresponding to an optical band gap of 2.25 eV. Figure 3 presents the gate-voltage (V_{GS}) dependent drain-source current (I_{DS}) characteristics of the fabricated bottom-gate Cu_2O TFTs after post-deposition annealing with a temperature of 800 °C, in contrast to those measured from the as-deposited films.

The measured I-V data show that the fabricated devices demonstrate clear p-channel behaviour with an increase of I_{DS} for negative V_{GS} . The I_{ON}/I_{OFF} ratio and $I_{DS,MAX}$ with the as-deposited film and with various annealing temperatures are summarized in table 1. Although I_{OFF} caused by defects and minority carriers (electrons) [26] should be improved, we note that the fabricated device with Cu_2O film annealed at 800 °C exhibits the highest I_{ON}/I_{OFF} ratio and $I_{DS,MAX}$ while the fabricated devices annealed at other temperatures have relatively poor electrical performance. It is noteworthy that high temperature annealing after film deposition gives rise to an improvement in film crystallinity and a reduction of copper vacancies in band tail states near E_V

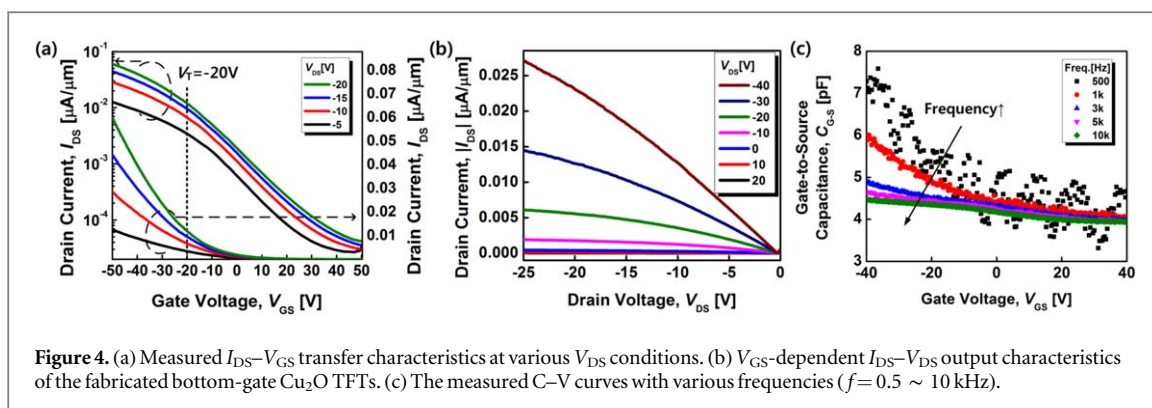


Figure 4. (a) Measured I_{DS} - V_{GS} transfer characteristics at various V_{DS} conditions. (b) V_{GS} -dependent I_{DS} - V_{DS} output characteristics of the fabricated bottom-gate Cu_2O TFTs. (c) The measured C-V curves with various frequencies ($f = 0.5 \sim 10$ kHz).

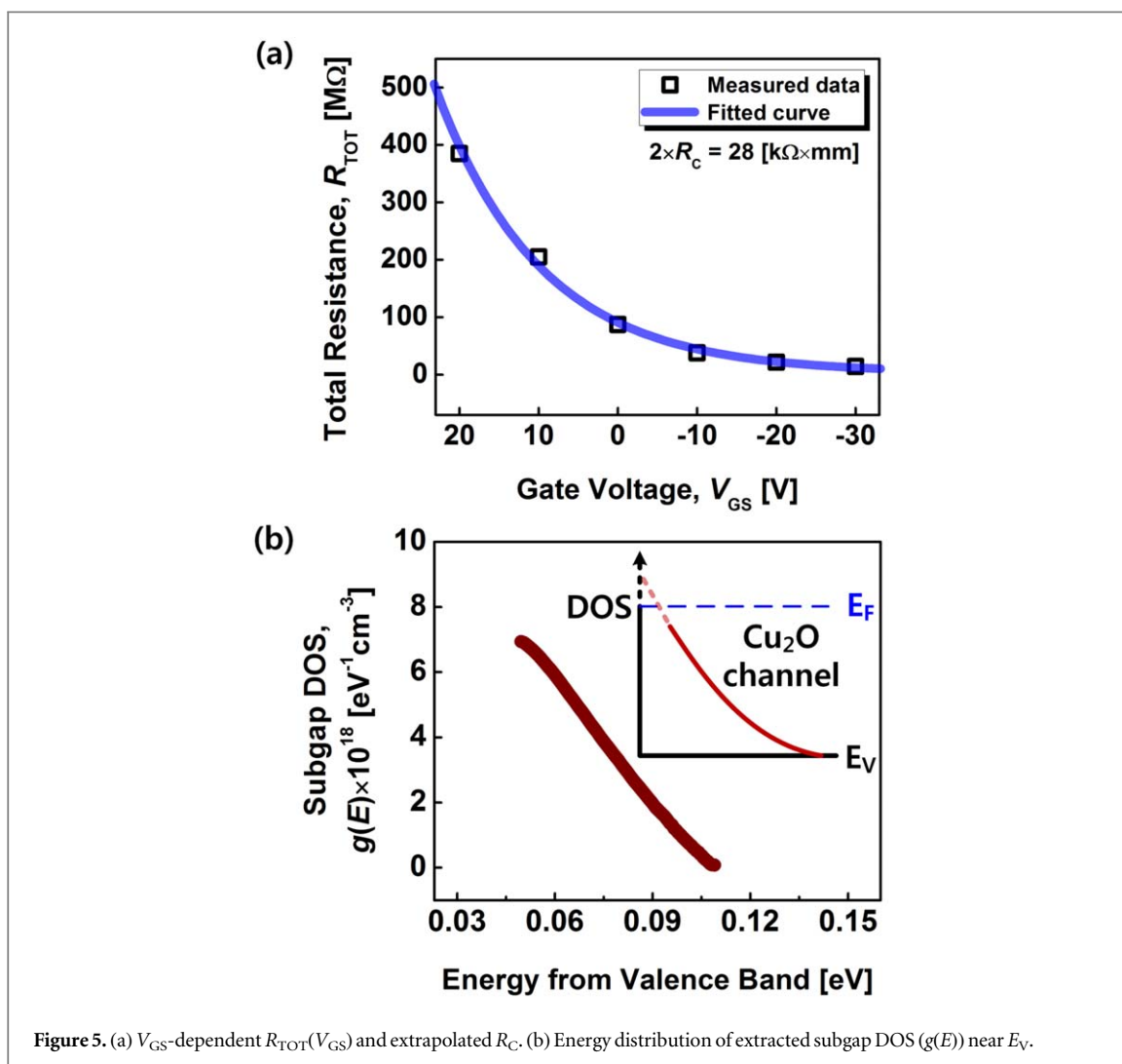


Figure 5. (a) V_{GS} -dependent $R_{TOT}(V_{GS})$ and extrapolated R_C . (b) Energy distribution of extracted subgap DOS ($g(E)$) near E_V .

Table 1. Device parameters with various post-deposition annealing temperatures.

$@V_{DS} = -20 \text{ V}$	I_{ON}/I_{OFF}	$I_{DS,MAX} [\mu\text{A } \mu\text{m}^{-1}]$
As-dep	—	2×10^{-4}
700 °C	$\sim 9 \times 10^1$	3×10^{-2}
800 °C	$\sim 2 \times 10^3$	6×10^{-2}
900 °C	$\sim 5 \times 10^1$	4×10^{-2}

[12]. The measured $I_{DS}-V_{GS}$ transfer and $I_{DS}-V_{DS}$ output characteristics of the fabricated bottom-gate Cu_2O TFTs are shown in figures 4(a) and (b), respectively.

Furthermore, the capacitance between the gate and the short circuited S/D in the p-channel Cu_2O TFT under the accumulation mode was characterized using an Agilent E4980A precision LCR meter. The frequency dependent capacitance-voltage (C-V) characteristics over the frequency range from 500 Hz to 10 kHz for the gate-to-source/drain configuration are shown in figure 4(c). Also, the measured capacitance value increases as V_{GS} increases in the negative direction. The results show the clear evidence for hole accumulation in the Cu_2O film ($V_{GS} < 0$). Especially, large frequency dispersion is attributed to capture-emission events occurring in both oxide bulk and interface with a contribution of large contact resistance (R_C) in S/D regions.

The R_C is obtained from extrapolated V_{GS} -dependent total series resistance ($R_{TOT}(V_{GS})$) as presented in figure 5(a). In the fabricated p-type Cu_2O TFTs, a quantitative analysis of the $g(E)$ over the bandgap is a significant issue when estimating the device instability which can be affected by film quality [27]. As shown in figure 5(b), we obtained $g(E)$ of $7.2 \times 10^{18} \text{ eV}^{-1} \text{ cm}^{-3}$ over the subgap energy ranges using V_{GS} -dependent ideality factor obtained from the subthreshold region of the measured $I_{DS}-V_{GS}$ curve [28]. Although we successfully demonstrated the fabrication and performance of PEALD Cu_2O TFTs, there still remain challenges in achieving higher mobility, better switching behaviors, and lower R_C in ultrathin p-type Cu_2O films. These issues are generally observed in the reported work related to p-type oxide transistors [11–16, 22]. More comprehensive study in particularly related to film growth and further device development are still under way.

4. Conclusion

In this work, we have developed a PEALD process to produce p-type Cu_2O films and demonstrated bottom-gate TFTs. P-type Cu_2O films are an important material building block for TMO-based BEOL transistors and circuits. The deposited Cu_2O thin-films with 12 nm thickness exhibited a high transparency of approximately 90%. Through post-deposition annealing at a temperature of 800 °C, the Cu_2O TFTs have a lower OFF-state current and a larger I_{ON}/I_{OFF} current ratio of 2×10^3 . These ultrathin and transparent Cu_2O TFTs fabricated with PEALD process could be a promising candidate for key devices for BEOL transistors in the hyper-scaled transistor era.

Acknowledgments

This work was supported in part by ASCENT, one of six centers in JUMP, a Semiconductor Research Corporation (SRC) program sponsored by DARPA. This work was also supported in part by the Office of Naval Research's Naval Enterprise Partnership Teaming with Universities for National Excellence (under Grant N00014-15-1-2833), Basic Science Research Program through the National Research Foundation of Korea (NRF) funded by the Ministry of Education (under Grant 2018R1A6A3A03013435), and the U.S. National Science Foundation for the TEM effort (DMR-1565822).

Data availability statement

All data that support the findings of this study are included within the article (and any supplementary files).

ORCID iDs

Hagyoul Bae  <https://orcid.org/0000-0002-2462-4198>

Haiyan Wang  <https://orcid.org/0000-0002-7397-1209>

Dmitry Zemlyanov  <https://orcid.org/0000-0002-1221-9195>

References

- [1] Fortunato E, Figueiredo V, Barquinha P, Elamurugu E, Barros R, Gonçalves G, Park S-H K, Hwang C-S and Martins R 2010 *Appl. Phys. Lett.* **96** 192102
- [2] Matsuzaki K, Nomura K, Yanagi H, Kamiya T, Hirano M and Hosono H 2008 *Appl. Phys. Lett.* **93** 202107
- [3] Al-Jawhari H A 2015 *Mater. Sci. Semicond. Process.* **40** 241
- [4] Wang Z, Nayak P K, Caraveo-Frescas J A and Alshareef H N 2016 *Adv. Mater.* **28** 3831
- [5] Salahuddin S, Ni K and Datta S 2018 *Nat. Electron.* **1** 442
- [6] Datta S, Dutta S, Grisafe B, Smith J, Srinivasa S and Ye H 2019 *IEEE Micro* **39** 8
- [7] Shijeesh M R, Mohan P A and Jayaraj M K 2020 *J. Electron. Mater.* **49** 537

- [8] Martins R, Nathan A, Barros R, Pereira L, Barquinha P, Correia N, Costa R, Ahnood A, Ferreira I and Fortunato E 2011 *Adv. Mater.* **23** 4491
- [9] Minami T, Miyata T and Nishi Y 2016 *Sol. Energy Mater. Sol. Cells* **147** 85
- [10] Tahir D and Tougaard S 2012 *J. Phys.: Condens. Matter* **25** 175002
- [11] Al-Jawhari H A and Caraveo-Frescas J A 2013 *Adv. Mater. Res.* **856** 215
- [12] Han S, Niang K M, Rughoobur G and Flewitt A J 2016 *Appl. Phys. Lett.* **109** 173502
- [13] Jeong C-Y, Sohn J, Song S-H, Cho I-T, Lee J-H, Cho E-S and Kwon H-I 2013 *Appl. Phys. Lett.* **102** 082103
- [14] Pattanasattayavong P, Thomas S, Adamopoulos G, McLachlan M A and Anthopoulos T D 2013 *Appl. Phys. Lett.* **102** 163505
- [15] Kim S Y, Ahn C H, Lee J H, Kwon Y H, Hwang S, Lee J Y and Cho H K 2013 *ACS Appl. Mater. Interfaces* **5** 2417
- [16] Zou X, Fang G, Yuan L, Li M, Guan W and Zhao X 2010 *IEEE Electron Device Lett.* **31** 827
- [17] Lee S-Y, Choi S-H and Park C-O 2000 *Thin Solid Films* **359** 261
- [18] Liao L et al 2001 *Appl. Surf. Sci.* **174** 177
- [19] Lim B S, Rahtu A and Gordon R G 2003 *Nat. Mater.* **2** 749
- [20] Napari M et al 2020 *ACS Appl. Mater. Interfaces* **13** 4156
- [21] Bae H et al 2019 *ACS Omega* **4** 20756
- [22] Kwon J-D, Kwon S-H, Jung T-H, Nam K-S, Chung K-B, Kim D-H and Park J-S 2013 *Appl. Surf. Sci.* **285** 373
- [23] Maeng W, Lee S-H, Kwon J-D, Park J and Park J-S 2016 *Ceram. Int.* **42** 5517
- [24] Kim H, Lee M Y, Kim S-H, Bae S I, Ko K Y, Kim H, Kwon K-W, Hwang J-H and Lee D-J 2015 *Appl. Surf. Sci.* **349** 673
- [25] Potts S E, Keuning W, Langereis E, Dingemans G, van de Sanden M C M and Kessels W M M 2010 *J. of Electrochem. Soc.* **157** 66
- [26] Han S and Flewitt A J 2017 *IEEE Electron Device Lett.* **38** 1394
- [27] Park I-J, Jeong C-Y, U M, Song S-H, Cho I-T, Lee J-H, Cho E-S and Kwon H-I 2013 *IEEE Electron Device Lett.* **34** 647
- [28] Jun S, Jo C, Bae H, Choi H, Kim D H and Kim D M 2013 *IEEE Electron Device Lett.* **34** 641